Desalination and Water Treatment
www.deswater.com
doi: 10.1080/19443994.2015.1033474

57 (2016) 10246–10260
May

Taylor & Francis
Taylor & Francis Group

Adsorption of crystal violet dye from aqueous solution onto chemically treated *Artocarpus odoratissimus* skin: equilibrium, thermodynamics, and kinetics studies

Linda B.L. Lim[a,*], Namal Priyantha[b,c], Tasneem Zehra[a], Cheow Wei Then[a], Chin Mei Chan[a]

[a]*Faculty of Science, Department of Chemistry, Universiti Brunei Darussalam, Jalan Tungku Link, Gadong, Negara Brunei Darussalam, Tel. +673 8748010; emails: linda.lim@ubd.edu.bn (L.B.L. Lim), if_tz@hotmail.com (T. Zehra), jaeycw@hotmail.com (C.W. Then), chinmei.chan@ubd.edu.bn (C.M. Chan)*
[b]*Faculty of Science, Department of Chemistry, University of Peradeniya, Peradeniya, Sri Lanka, email: namal.priyantha@yahoo.com (N. Priyantha)*
[c]*Postgraduate Institute of Studies, University of Peradeniya, Peradeniya, Sri Lanka*

Received 28 November 2014; Accepted 20 March 2015

ABSTRACT

In this study, the feasibility of utilizing *Artocarpus odoratissimus* skin ("Tarap" skin or TS) as a potential adsorbent for the removal of crystal violet dye was investigated. X-ray fluorescence, Fourier Transform Spectroscopic, and scanning electron microscopic investigation of TS and its NaOH-treated form (NaOH-TS) before and after interaction with crystal violet (CV) cationic dye indicate that the dye shows a strong affinity toward the adsorbent, which is enhanced upon the treatment with a NaOH solution. Decrease in the concentration of metal ions on the TS/NaOH-TS is indicative of the contribution of an ion-exchange mechanism owing to the positive charge of CV molecules. Comparison of experimental adsorption curves with calculated curves point the way toward the agreement with the Langmuir isotherm among the six models tested (Langmuir, Freundlich, Temkin, Dubinin–Radushkevich, Redlich–Peterson, and Sips) under optimized conditions with maximum adsorption capacity of 118 mg g^{-1} for TS which is significantly enhanced to 195 mg g^{-1} upon treatment with NaOH. Kinetics studies support pseudo-second-order and intra-particle diffusion mechanisms. Based on the thermodynamic parameters such as enthalpy (ΔH°), entropy (ΔS°), and Gibbs free energy changes (ΔG°), the sorption of CV dye onto TS and NaOH-TS is a spontaneous and endothermic process.

Keywords: *Artocarpus odoratissimus* skin; Crystal violet; Adsorption; Equilibrium isotherms; Kinetics

1. Introduction

As a result of rapid increase in the world's population, expansion of industrialization is needed to cater to the global needs. This industrialization boom comes at the expense of the environment as more and more pollutants are being discharged into air and water systems. There is an urgent need to investigate environmental pollution, as it poses a severe risk of damages to the eco-systems, in particular, to human health. Emergence of various methods to remove these

*Corresponding author.

pollutants has occurred over the past decades, and such methods have been extensively reviewed [1,2]. One attractive method that has caught the attention of researchers is the adsorption owing to its inherent advantages, such as simplicity and efficiency. The use of activated carbon as an adsorbent, albeit effective, can be costly. Hence, recent attention has been turned toward the search for new low-cost adsorbents as a replacement. This has led to the discovery of adsorbents such as fruit wastes [3,4], peat [5], plant wastes [6], fungus [7], and other adsorbents [8,9] for the removal of various pollutants.

Artocarpus odoratissimus, locally known as "Tarap", is a popular tropical seasonal fruit in Brunei Darussalam. The fruit itself is made up of the inedible skin and core, and the edible flesh and seeds. About half the fruit is discarded as waste without being utilized [10]. It was already shown that the core and/or skin of *A. odoratissimus* can be used as effective adsorbents for the removal of Cd (II) and Cu(II) metal ions [11] and cationic methylene blue and methyl violet 2B dyes [12]. Further, crystal violet has been removed by other adsorbents, such as *Artocarpus altilis* (breadfruit) [13], date palm fiber [14], cocoa (*Theobroma cacao*) shell [15], *Artocarpus heterophyllus* (jackfruit) leaf powder [16], hen feathers [17], and eggshells [18].

As an extension to these findings, this present study focuses on the adsorption ability of *A. odoratissimus* skin (TS) to remove crystal violet (CV) dye from aqueous solutions. Crystal violet (CV), a basic dye, also known as gentian violet and methyl violet 10B, belongs to the class of triarylmethane dyes. It is widely used in paints, printing ink, and textiles. It is non-biodegradable and can persist in a variety of environments. Therefore, it is essential to remove CV from wastewaters before their discharge for environmental safety. To date, there has been no report on the use of *A. odoratissimus* adsorbent for the removal of CV. Further, chemical pretreatment to further improve adsorption capacities of TS is also reported. Alkali and acid treatments are one of the commonly employed chemical treatment techniques for the purpose of improving adsorption properties of adsorbents. These treatments have been reported for its substantial influence on morphological properties causing changes in pore structure as well as molecular and chemical changes [19–22]. In present study, NaOH treatment is used. X-ray fluorescence (XRF) reveals presence of Na in TS after NaOH treatment which is not observed in untreated TS. The objective of this work is to study the adsorption of CV onto TS and NaOH-treated TS. The effects of contact time, ionic strength, and pH have been investigated. Adsorption isotherms, kinetics, and thermodynamics parameters are also evaluated and reported.

2. Materials and methods

2.1. Sample preparation

A. odoratissimus fruits were randomly purchased from the local open markets. The skin was separated from the fruits and was oven-dried at 60°C to constant mass. Dried *A. odoratissimus* skin (TS) was blended and sieved to obtain desired particle sizes (355–850 μm) and stored in a desiccator prior to use. The pretreatment of TS was carried out with NaOH (1.0 mol L^{-1}) and named as NaOH-TS.

2.2. Chemicals and reagents

Crystal violet ($C_{25}H_{30}N_3Cl$) dye was purchased from Sigma-Aldrich Corporation. Its stock solution of 1,000 mg L^{-1} was prepared by dissolving the required amount in distilled water. Other concentrations of CV were obtained by dilution of the stock solution. Solution pH was adjusted using NaOH and HNO_3 purchased from Fluka (0.1 M for major adjustments of pH, while 0.01 M for minor adjustments). All chemicals were used without further purification.

2.3. Instrumentation

Shimadzu UV-1601PC UV–visible spectrophotometer (UV–vis) was used to record absorbance measurements at the λ_{max} of 590 nm to determine the concentration of CV in all solutions. Functional group characterization of TS before and after treatment with CV dye was carried out using FTIR spectrophotometer (Shimadzu Model IRPrestige-21). Stuart orbital shaker used for agitation of the solution was set at 250 rpm. Scanning Electron Microscope (SEM) images of TS samples were obtained using Tescan Vega XMU SEM and XRF measurements were taken on PANalytical Axios^{max} instrument for quantitative determination of elements.

2.4. Batch experimental procedure

Batch experiments were carried out by mixing 0.10 g of adsorbent with 50.0 mL of CV solution of known concentration for all experiments. Effect of contact time was investigated by agitating the mixtures followed by filtration at predetermined time intervals (30–240 min). Parameters such as pH (2–8) and ionic strength were also investigated. Ionic strength studies

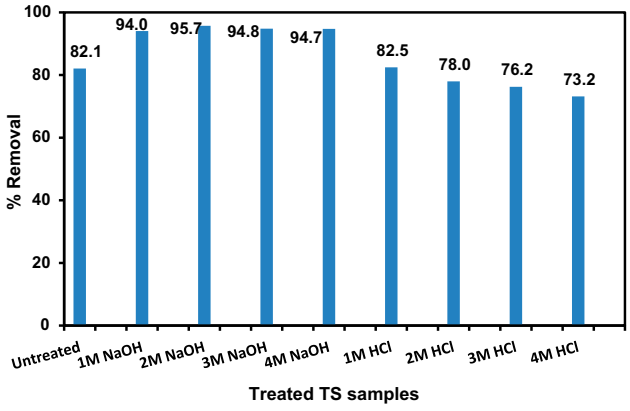

Fig. 1. Effect of pretreatment on removal of CV by TS (concentration of CV: 100 mg L^{-1}; volume: 50.0 mL; mass of TS: 0.10 g).

were conducted by mixing 50.0 mL aliquots solutions containing potassium nitrate of different concentrations (0.1–1.8 mol L^{-1}) and 0.10 g samples of adsorbent. The mixture was filtered and the filtrate was analyzed for its CV content. Thermodynamics studies were carried out at different temperatures (298, 314, 324, 334, and 344 K).

The Langmuir, Freundlich, Temkin, Dubinin–Radushkevich (D–R), Redlich–Peterson (R–P), and Sips isotherm models were used for describing the adsorption process at equilibrium. Lagergren's first-order, pseudo-second-order, Weber–Morris intra-particle diffusion, and Elovich models were used for kinetics studies. All experiments were carried out in duplicate, and the results were taken as an average.

Eq. (1) was used to calculate the amount of dye adsorbed per gram of adsorbent, q_e (mg g^{-1}):

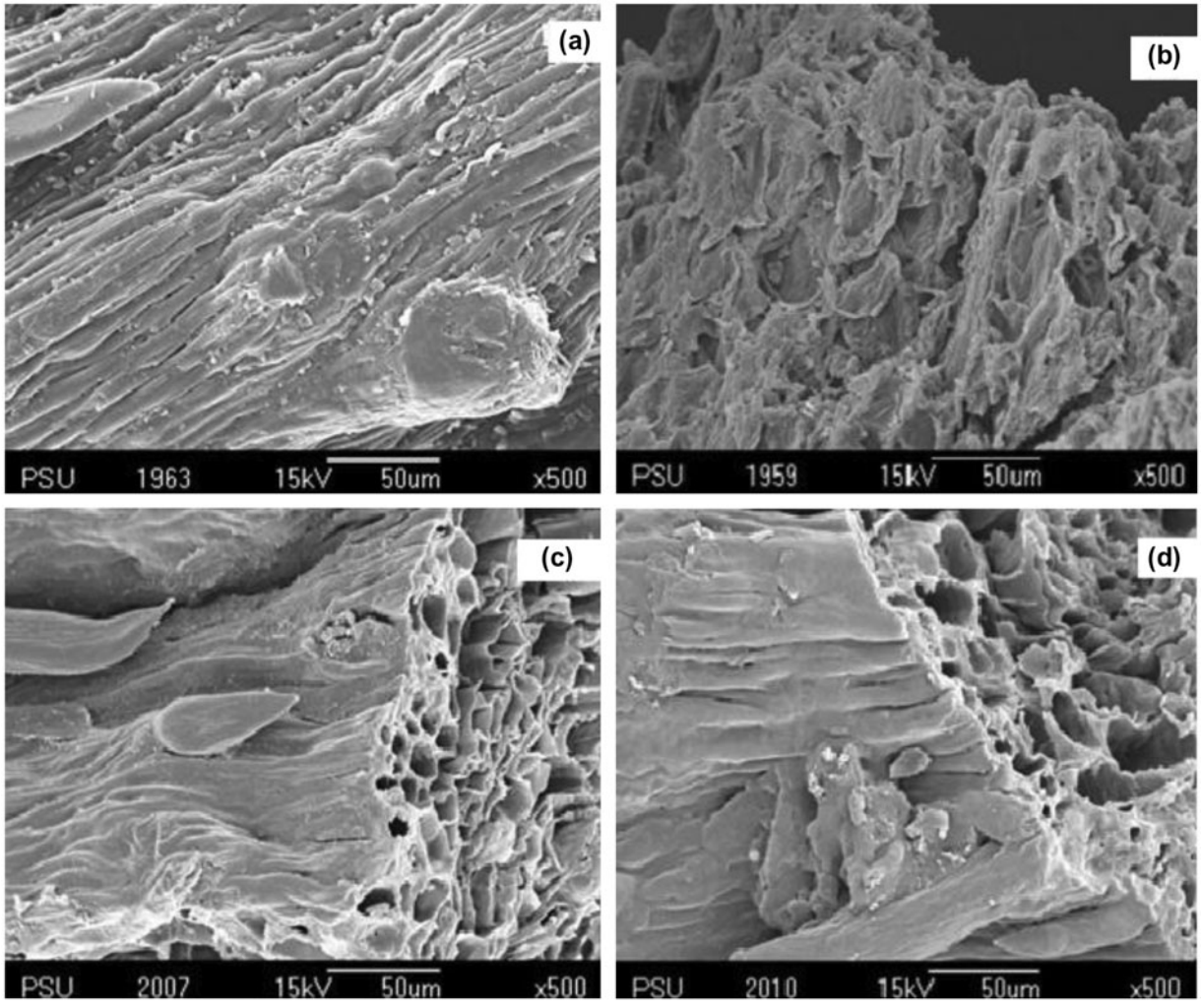

Fig. 2. Surface morphology by SEM at 502× magnification (a) TS, (b) TS with CV, (c) TS-NaOH, and (d) NaOH-TS with CV.

$$q_e = \frac{(C_i - C_e)\,V}{m} \quad (1)$$

$$\%\ \text{removal} = \frac{(C_i - C_e)\ \times 100}{C_i} \quad (2)$$

where C_i is the initial dye concentration (mg L^{-1}), C_e is the equilibrium dye concentration (mg L^{-1}), V is the volume of CV solution used (L), and m is the mass of adsorbent used (g). The percentage removal of the dye is represented by:

2.5. Determination of zero point charge (pH_{PZC})

The zero point charge was determined using the salt addition method. For this, 0.1 M KNO_3 solutions,

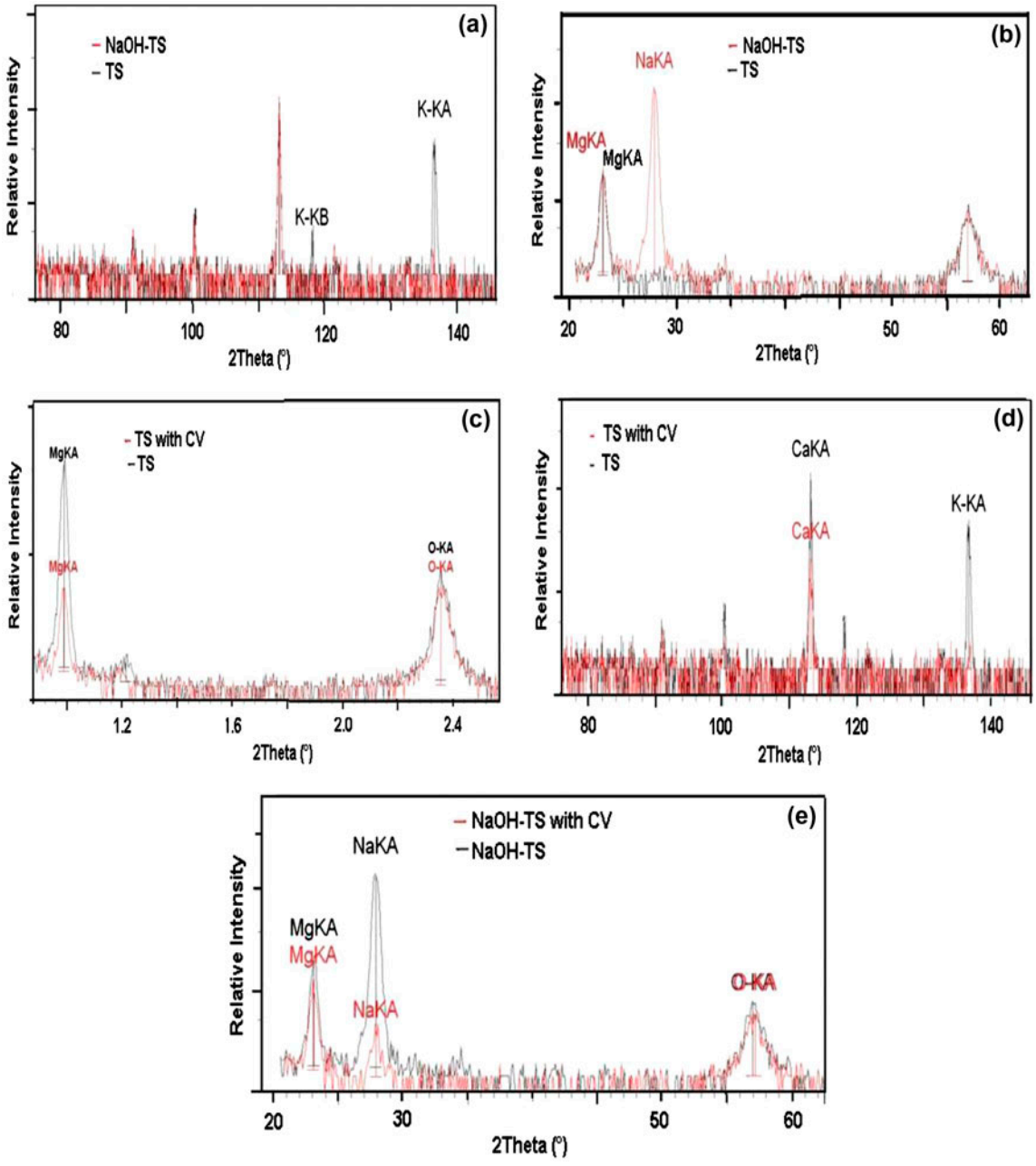

Fig. 3. XRF spectra of TS and NaOH-TS: (a) and (b) showing K, Mg, and Na peaks in TS (-) and NaOH-TS (▬); (c) and (d) showing Mg, Ca, and K peaks in TS (-) and TS treated with CV (▬); (e) showing Mg and Na peaks in NaOH-TS (-) and NaOH-TS treated with CV (▬).

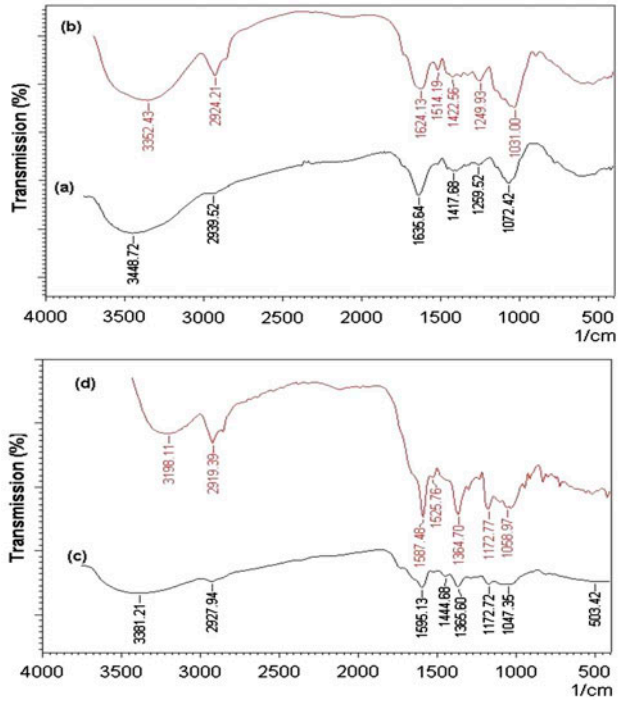

Fig. 4. FTIR Spectra (a) TS, (b) NaOH-TS, (c) TS with CV, and (d) NaOH-TS with CV.

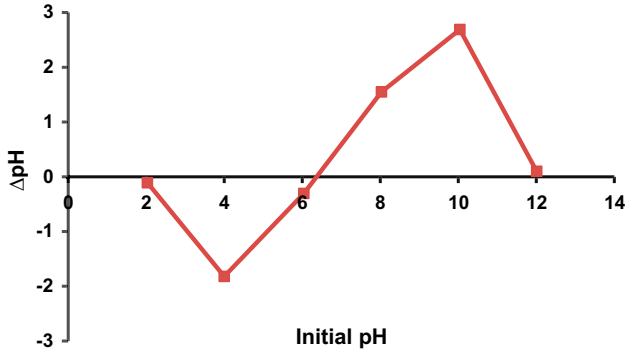

Fig. 5. Variation of ΔpH vs. initial pH for the determination of point of zero charge for NaOH-TS.

whose initial pH values were adjusted between 2 and 12, were mixed with 0.10 g of adsorbent for 24 h. After 24 h of shaking, the pH values of the suspensions were measured.

3. Results and discussion

3.1. Tarap skin pretreatment

Treatment of TS with 1.0 M NaOH followed by treatment with CV for a randomly selected shaking time and a settling time leads to an increase in the extent of removal of CV from 52.1 to 94.0%. Further increase in the concentration of the NaOH solution does not significantly enhance the removal ability of TS, and hence the treatment was done with 1.0 M NaOH in future experiments. Although the base treatment enhances the extent of removal of CV, acid

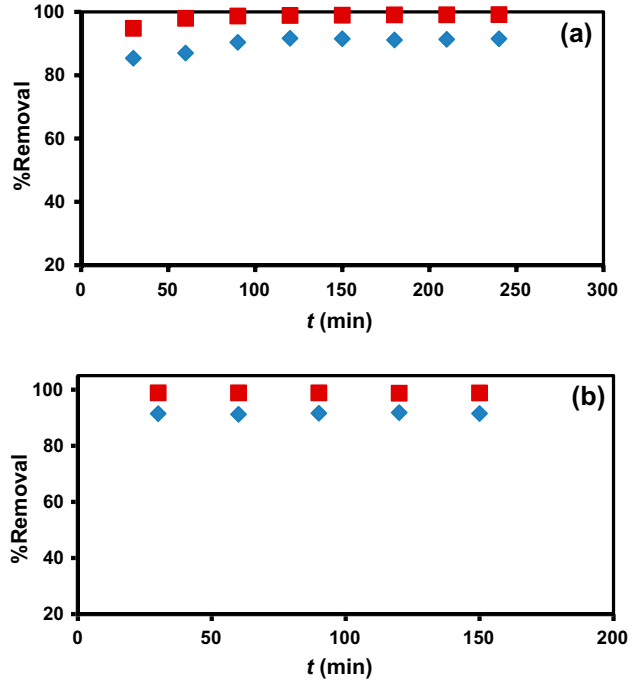

Fig. 6. Effect of shaking time (a) and settling time (b) on the removal of CV by TS (♦) and NaOH-TS (■) (concentration of CV: 10 mg L^{-1}; volume: 50.0 mL; mass of adsorbent: 0.10 g).

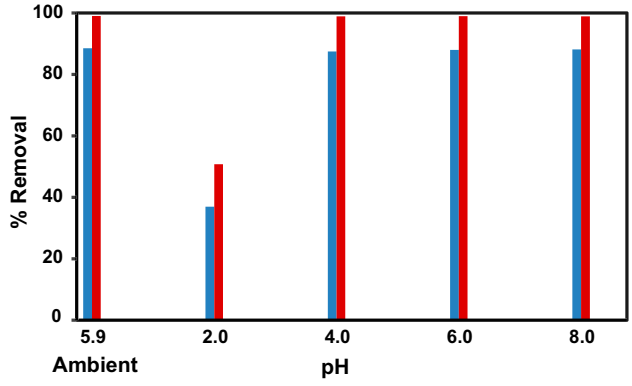

Fig. 7. Effect of medium pH on the removal of CV by TS (■) and NaOH-TS (■) (concentration of CV: 100 mg L^{-1}; volume: 50.0 mL; mass of adsorbent: 0.10 g; shaking time: 2.5 h; settling time: 30 min).

treatment leads to an opposing effect, probably due to the repulsion between positively charged CV and positively charged TS surface owing to the acid treatment. Thus, acid treatment was not considered as an effective pretreatment method (Fig. 1).

3.2. Characterization of adsorbents

The fibrous structure of TS is clearly seen in the SEM image (Fig. 2(a)), where space between fibers may serve as adsorption sites [12]. The fibrous structure is damaged and large pores are formed upon treatment with NaOH solution as evident in the SEM image (Fig. 2(c)). These pores serve as binding sites, and especially, pores of larger sizes would be able to trap big molecules, such as crystal violet.

Treatment with NaOH solutions would therefore provide favorable conditions for enhancing affinity of TS toward CV. Images after CV adsorption (Fig. 2(b) and (d)) show partially filled pores indicating that the surface is covered with CV.

XRF analysis of TS indicates the presence of many metals including K, Mg, and Ca. Treatment of TS by CV has decreased the levels of Mg and K significantly (Fig. 3(c) and (d)), suggesting that cationic CV would be able to replace such metal ions, probably similar to an ion-exchange mechanism. Treatment of TS with NaOH solution leads to the exchange of K^+ ions by Na^+ ions, and therefore NaOH-TS does not have detectable K, but has a high concentration of Na (Fig. 3(a) and (b)). The Na present in NaOH-TS is significantly decreased upon treatment with CV due to the same mechanism as explained earlier (Fig. 3(e)).

Based on FTIR spectra (Fig. 4), functional groups that are likely to be responsible for the adsorption of CV are the hydroxyl/amino and carboxylic acid groups, and these can be confirmed by the shift in wavelengths of these groups upon adsorption of CV. A peak at 3,449 cm^{-1} (corresponding to the hydroxyl/amino group) in TS shifted to a lower value 3,381 cm^{-1}. This peak was observed at 3,352 cm^{-1} in NaOH-TS which was shifted to 3,198 cm^{-1} upon CV adsorption. Shifts were also observed from 1,635 and 1,624 cm^{-1} to 1,595 and 1,587 cm^{-1} upon treating with CV for TS and NaOH-TS, respectively, indicating the involvement of C=O of carboxylic acid.

3.3. Determination of pH at point of zero charge (pH_{PZC})

Point of zero charge of NaOH-TS was observed at pH of 6.4 (Fig. 5), which is much higher than the pH_{PZC} reported for TS [12]. This can be explained by considering the fact that NaOH treatment acts as an acid–base reaction converting acidic functionalities to corresponding anionic forms, providing a negatively charged surface on NaOH-TS.

3.4. Optimization of adsorption parameters

Effect of four parameters on the extent of removal of CV was investigated in this study to provide the optimal conditions for its adsorption on TS and NaOH-TS, namely shaking time and settling time (i.e. contact time), medium pH, and ionic strength. Based on the variation of the extent of removal vs shaking time plot as shown in Fig. 6(a), it is clear that more than 80% of the dye was adsorbed by both TS types within the first 60 min, which could be attributed to the availability of vacant sites for dye adsorption. However, over time, as these sites become occupied by the dye molecules, the rate of adsorption decreases

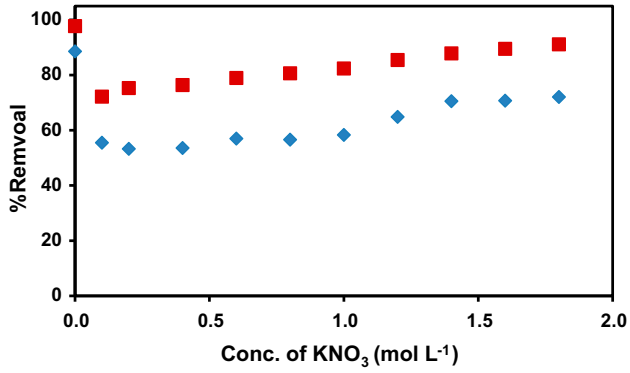

Fig. 8. Effect of ionic strength on CV removal by TS (♦) and NaOH-TS (■) (concentration of CV: 100 mg L^{-1}; volume: 50.0 mL; mass of adsorbent: 0.10 g; shaking time: 2.5 h; settling time: 30 min).

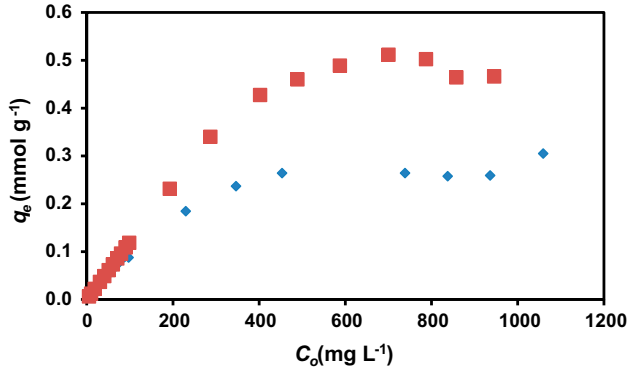

Fig. 9. Adsorption capacity of TS (♦) and NaOH-TS (■) (concentration of dye: 5–1,000 mg L^{-1}; volume of dye: 25 mL; mass of peat: 0.050 g).

and finally, the system reaches equilibrium. The system was then allowed to settle for the establishment of complete equilibrium. No significant variation on the extent of dye removal was observed beyond 30 min (Fig. 6(b)). The optimum shaking time was set at 2.5 h followed by a settling time period of 30 min.

Higher removal by NaOH-TS as compared to TS can be attributed to the columbic attraction of positively charged CV species to negatively charged surface of NaOH-TS formed as a result of base treatment.

It was found that the highest extent of removal of CV was at its ambient pH of 5.9. The lowest removal at pH 2 (Fig. 7) can be explained by the cationic nature of CV dye which would result in electrostatic repulsion with predominantly positively charged surface of TS, since this pH was lower than its point of zero charge of 4.4 as reported earlier [12] and of 6.4 for NaOH-TS reported in this study. Furthermore, there was competition between cationic CV dye molecules and H^+ ions present in high concentration at low pH. As the pH increases from pH 2 to pH 4, the amount of CV adsorbed is increased, and thereafter, only a slight increase was observed up to pH 8. Hence, the ambient pH, which gave 88.5 and 99.0% removal by TS and NaOH-TS, respectively, provided the optimum condition for the removal of CV. Therefore, no pH adjustment was carried out in this study.

As it is expected that ionic interactions play a major role in removing CV from solution by TS, effect of the ionic strength of the medium would also be an

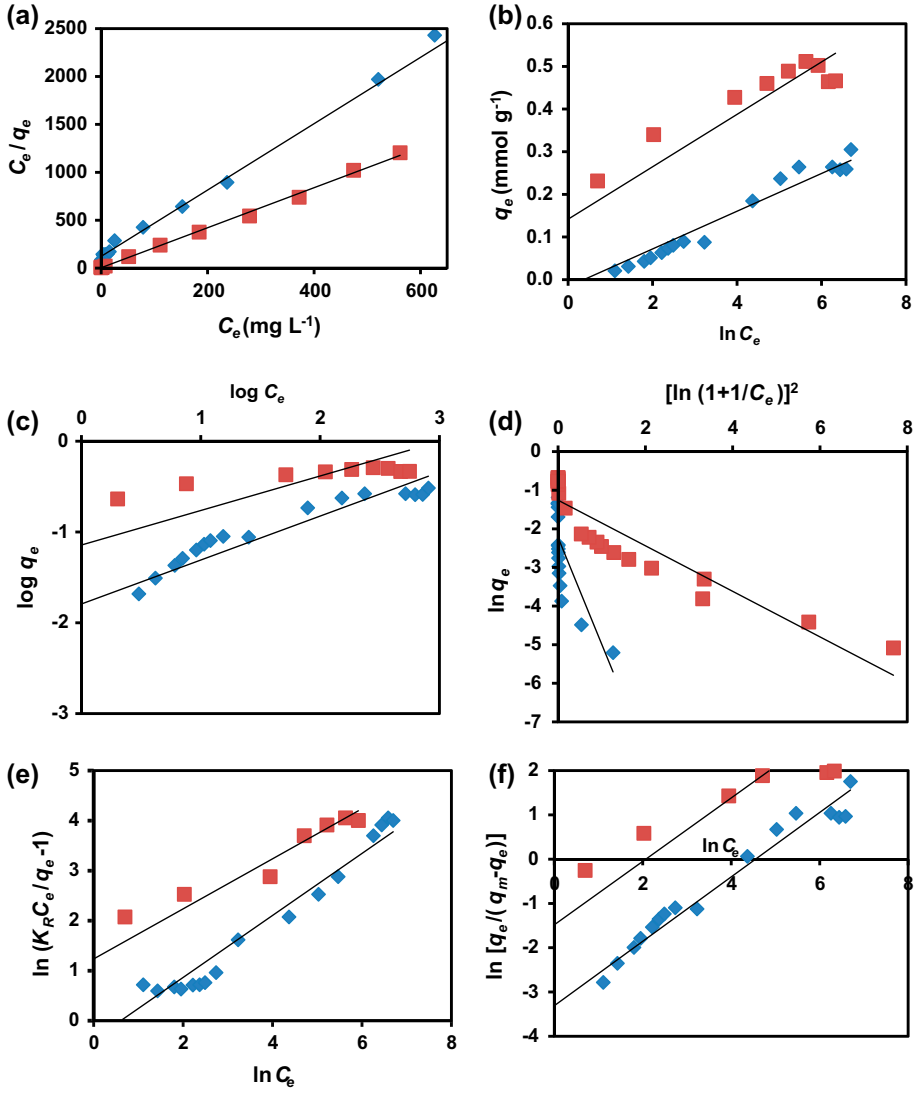

Fig. 10. Linear plots of (a) Langmuir, (b) Freundlich, (c) Temkin, (d) D–R, (e) R–P, and (f) Sips. TS (♦) and NaOH-TS (■) (concentration of dye: 5–1,000 mg L^{-1}; volume of dye: 25 mL; mass of peat: 0.050 g).

Table 1
Isotherm parameters determined from different models

Model	Parameters	Value	
		TS	NaOH-TS
Langmuir	q_{max} (mg g^{-1})	118	195
	K_L (L $mmol^{-1}$)	0.03	0.50
	R^2	0.988	0.998
Freundlich	K_F (mmol g^{-1})	0.02	0.07
	n	2.07	2.63
	R^2	0.919	0.817
Temkin	K_T (L $mmol^{-1}$)	0.68	10.03
	b_T (kJ mol^{-1})	55.55	40.29
	R^2	0.940	0.970
Dubinin–Radushkevich (D–R)	q_{max} (mg g^{-1})	44	116
	β (mol^2 J^2)	3.71×10^{-7}	9.6×10^{-8}
	E (kJ mol^{-1})	1.16	2.28
	R^2	0.535	0.854
Redlich–Peterson	K_R(L g^{-1})	0.02	0.66
	n	0.62	0.65
	a_R (L $mmol^{-1}$)	0.69	7.53
	R^2	0.957	0.923
Sips	q_{max} (mg g^{-1})	146.1	216.3
	K_S (L $mmol^{-1}$)	0.04	0.23
	n	1.36	1.40
	R^2	0.973	0.946

important variable. The extent of removal of CV by TS, as shown in Fig. 8, was decreased from 88.6 to 55.5% in 0.10 M KNO_3 medium, further supporting that ion exchange does have a strong contribution. Similar decrease (from 97.8 to 72.2%) in the extent of removal was observed for NaOH-TS as well. However, increase in the ionic strength beyond 0.10 M KNO_3 results in a slow increase in the dye removal. At low concentration of ionic strength, decrease in the extent of adsorption could be due to screening effect of electrolyte. Counter ions in the medium surround the adsorption sites, lose their charge, and weaken the binding force by an electrostatic interaction between adsorbent surface and dye [23]. In another aspect, presence of salt can increase the degree of dissociation of a dye molecule by facilitating protonation [24]. Hence, adsorbent removes more dye molecules which are dissociated in ions and free for binding electrostatically onto the oppositely charged adsorbent surface [25]. The latter effect seems to be dominant with the increase in ionic strength (Fig. 8).

3.5. Adsorption isotherms

Adsorption systems can be investigated using different adsorption isotherms. Six isotherm models investigated in this study are Langmuir, Freundlich, Temkin, Dubinin–Radushkevich (D–R), Redlich–Peterson (R–P), and Sips models whose linearized relationships are given as,

Langmuir adsorption isotherm:

$$\frac{C_e}{q_e} = \frac{1}{K_L q_{max}} + \frac{C_e}{q_{max}} \tag{3}$$

Freundlich adsorption isotherm:

$$\log q_e = \frac{1}{n}\log C_e + \log K_F \tag{4}$$

Temkin adsorption isotherm:

$$q_e = \left(\frac{RT}{b_T}\right) \ln K_T + \left(\frac{RT}{b_T}\right) \ln C_e \tag{5}$$

Dubinin–Radushkevich (D–R) adsorption isotherm:

$$\ln q_e = \ln q_{max} - \beta\varepsilon^2 \tag{6}$$

where $\varepsilon = RT \ln\left(1 + \frac{1}{C_e}\right)$ and $E = \frac{1}{\sqrt{2\beta}}$

Redlich–Peterson (R–P) adsorption isotherm:

$$\ln\left(\frac{K_R C_e}{q_e} - 1\right) = n \ln C_e + \ln a_R \quad (7)$$

Sips adsorption isotherm:

$$\ln\left(\frac{q_e}{q_{\max} - q_e}\right) = \frac{1}{n}\ln C_e + \ln K_s \quad (8)$$

Fig. 9 shows the experimental adsorption points obtained from batch experiments performed using solutions of CV of concentrations ranging from 5 to 1,000 mg L^{-1} followed by optimum shaking and settling time. Fig. 9 clearly indicates a monolayer adsorption of CV by TS, which is further confirmed by the high linear regression of Langmuir isotherm model as compared to the Freundlich model.

The linear plots based on Eqs. (3)–(8) using the equilibrium concentrations were used to calculate the adsorption parameters of all isotherm models (Fig. 10). The values of parameters obtained from slopes and intercepts of linear regression plots are given in Table 1. The best correlation coefficients were, in decreasing order, Langmuir > Sips > R–P > Temkin > Freundlich > D–R for TS and Langmuir > Temkin > Sips > R–P > Freundlich > D–R for NaOH-TS.

Although, determination of the best isotherm model is possible through analysis of the regression coefficient (R^2); in this work, four different error functions were employed in order to discover the most suitable isotherm for representing the experimental data. Relationships for error analysis, namely, sum square error (SSE), hybrid fractional error function (HYBRID), sum of absolute error (EABS), and chi-square test (χ^2) are represented as follows,

$$\text{SSE: } \sum_{i=1}^{n}(q_{e,\text{calc}} - q_{e,\text{meas}})_i^2 \quad (9)$$

$$\text{HYBRID: } \frac{100}{n-p}\sum_{i=1}^{n}\left[\frac{(q_{e,\text{meas}} - q_{e,\text{calc}})^2}{q_{e,\text{meas}}}\right]_i \quad (10)$$

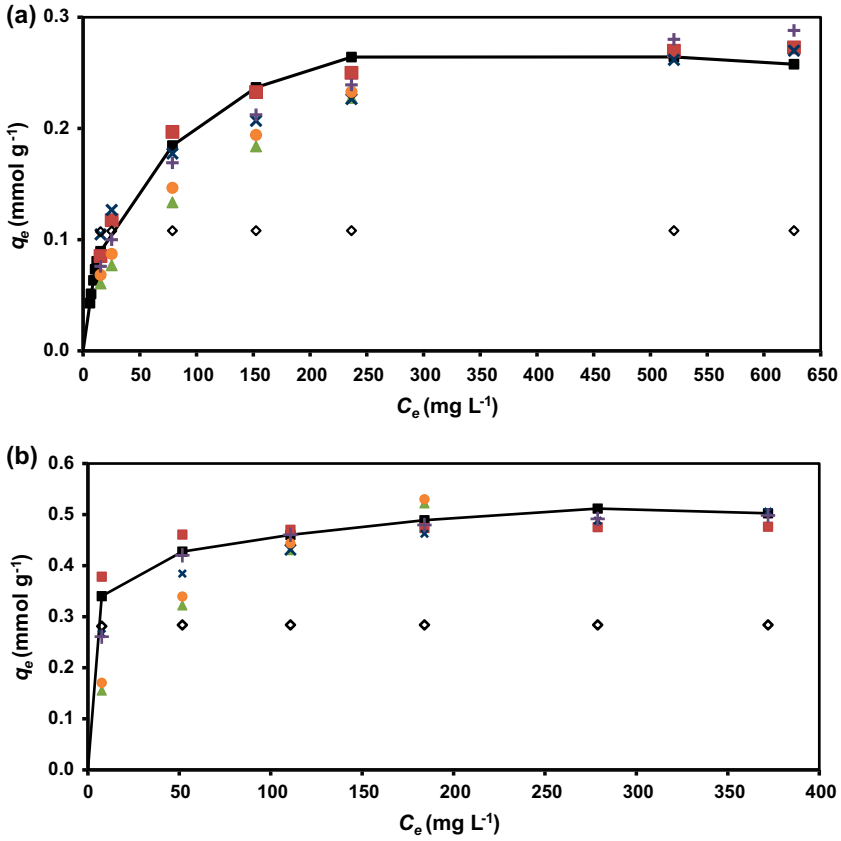

Fig. 11. Fitting of isotherm models: Experimental (■) data with simulated Langmuir (■), Freundlich (▲), Temkin (×), D–R (◇), R–P (+), Sips (+); (A) TS and (B) NaOH-TS. Experimental conditions: volume of solution: 50.0 mL; mass of adsorbent: 0.10 g; shaking time: 2.5 h; settling time: 30 min.

Table 2
Errors calculated for various isotherm models

Model	SSE	HYBRID	EABS	χ^2
TS				
Langmuir	0.003	0.14	0.17	0.02
Freundlich	0.054	1.80	0.69	0.29
Temkin	0.011	4.51	0.38	0.72
Dubinin–Radushkevich (D–R)	0.175	7.45	1.42	1.19
Redlich–Peterson	0.033	0.95	0.53	0.14
Sips	0.005	0.19	0.23	0.03
NaOH-TS				
Langmuir	0.01	0.49	0.38	0.09
Freundlich	0.31	4.84	1.63	0.87
Temkin	0.02	1.50	0.57	0.27
Dubinin–Radushkevich (D–R)	0.29	5.08	1.90	0.91
Redlich–Peterson	0.28	4.33	1.52	0.74
Sips	0.02	0.67	0.43	0.11

$$\text{EABS: } \sum_{i=1}^{n} \left| q_{e,\text{meas}} - q_{e,\text{calc}} \right| \tag{11}$$

$$\chi^2\text{: } \sum_{i=1}^{n} \frac{\left(q_{e,\text{meas}} - q_{e,\text{calc}}\right)^2}{q_{e,\text{meas}}} \tag{12}$$

where $q_{e,\text{meas}}$ is the experimental value, $q_{e,\text{calc}}$ is the calculated value, n is the number of data points in the experiment, and p is the number of parameters of the model. Also, the simulation is usually used in order to judge the reasonableness of the model. The simulated q_e values for each model, calculated from their non-linear forms, were plotted against equilibrium concentration and compared with experimental values obtained (Fig. 11).

Based on the factors, regression coefficient (R^2) being close to 1.000 (Table 1), good agreement between experimental and simulated nonlinear curve fitting and low overall error in different error function

Table 3
Comparison of adsorption capacity of TS and NaOH-TS for CV with other reported low-cost adsorbents

Adsorbent	$q_{\max}$ (mg g^{-1})	References
Artocarpus odoratissimus peel (TS)	118	This work
Artocarpus odoratissimus peel (NaOH-TS)	195	This work
Artocarpus heterophyllus leaf powder	43	[16]
Hen feathers	64	[17]
Eggshells	70	[18]
Citric acid-modified rice straw	81	[21]
H_2SO_4-modified sugarcane bagasse	148	[22]
Peat	108	[26]
NaOH-modified rice husk	45	[27]
Artocarpus altilis peel	146	[13]
Agaricus bisporus	22	[7]
Acid-activated sintering process red mud	60	[28]
Male flowers coconut tree:		[29]
—phosphoric acid activated	60	
—sulfuric acid activated	86	
Palm kernel	79	[30]
Treated ginger waste	65	[31]
Formosa papaya seed powder	86	[32]
Magnetic nanocomposite	118	[33]
kappa-carrageenan/PVA mixture	55	[34]

(Table 2), Langmuir adsorption isotherm is the most suitable for adsorption of CV on TS or NaOH-TS. The Langmuir isotherm estimates the maximum adsorption capacity corresponding to complete monolayer coverage on the surface of an adsorbent for any adsorbate.

Table 4
Equations for kinetic models in their linearized form

Kinetic models	Linear equations	
Pseudo-first-order	$\log(q_e - q_t) = \log(q_e) - \frac{k_1}{2.303}t$	(13)
Pseudo–second-order	$\frac{t}{q_t} = \frac{q}{k_2 q_e^2} + \frac{1}{q_e}t$	(14)
Weber–Morris intra-particle diffusion	$q_t = k_{id}t^{1/2} + C$	(15)
Elovich	$q_t = \frac{1}{b}\ln(ab) + \frac{1}{b}\ln t$	(16)

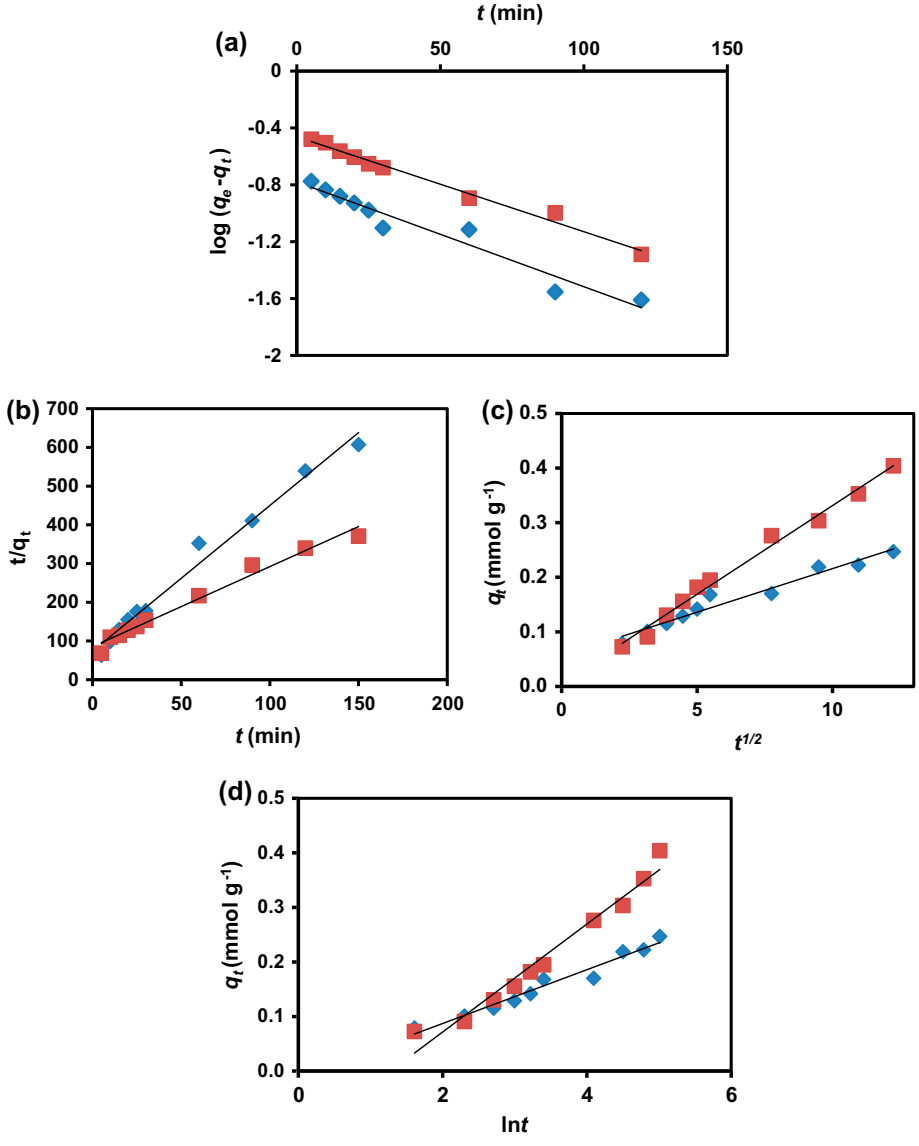

Fig. 12. Applicability of kinetics models to TS (♦) and NaOH-TS (■): (a) Pseudo-first-order model, (b) Pseudo-second-order model, (c) Intra-particle diffusion model, and (d) Elovich model.

Table 5
Parameters for kinetic models for adsorption of CV at 500 mg L^{-1}

Kinetics	TS	NaOH-TS
$q_{e,exp}$ (mmol g^{-1})	0.25	0.40
Pseudo-first-order		
k_1 (min^{-1})	0.02	0.02
$q_{e,calc}$ (mmol g^{-1})	0.17	0.34
R^2	0.946	0.987
Pseudo–second-order		
k_2 (g $mmol^{-1}$ min^{-1})	0.19	0.05
h (mmol g^{-1} min^{-1})	0.01	0.01
$q_{e,calc}$ (mmol g^{-1})	0.27	0.48
R^2	0.985	0.979
Intra-particle diffusion model		
k_{id} (mmol g^{-1} $min^{-1/2}$)	0.02	0.03
C (mmol g^{-1})	0.06	0.01
R^2	0.959	0.989
Elovich		
a (mmol g^{-1} min^{-1})	0.04	0.03
b (g $mmol^{-1}$)	20.24	10.10
R^2	0.964	0.966

The comparison of monolayer adsorption capacities of various adsorbents for CV such as acid-activated sintering process red mud [28], palm kernel [30], papaya seed powder [32], and *kappa*-carrageenan/PVA mixture [34] shows that TS and NaOH-TS have higher adsorption capacities for CV than many other reported adsorbents (Table 3). Being economical and easily available, TS and NaOH-TS would serve as effective adsorbents for the removal of CV from aqueous solution.

3.6. Kinetics studies on adsorption of CV

Four kinetic models, namely the pseudo-first-order, pseudo–second-order, Weber–Morris intra-particle diffusion, and the Elovich models were used to further elaborate the mode of sorption of CV on TS and NaOH-TS. Their equations are listed in Table 4, where q_e and q_t (mmol g^{-1}) are the amount of dye adsorbed at equilibrium and at time t (min), k_1 is the pseudo-first-order rate constant; k_2 is the pseudo-second-order rate constant; k_{id} is intra-particle diffusion rate constant; C gives idea about the thickness of boundary layer; a is the Elovich's initial sorption rate; and b is related to the extent of surface coverage and activation energy for chemisorption during any one experiment.

Pseudo-kinetic models require one of the concentrations of reactants to be in large excess. Hence, 500 mg L^{-1} CV was chosen for the kinetic studies. Fig. 12 shows plots for each kinetic model. All plots yielded straight lines.

All the models fit well to the experimental data. Table 5 shows parameters calculated for each kinetic model. Compared to the pseudo-first-order kinetics, the pseudo-second-order kinetics model gave a better linear coefficient where R^2 was close to unity for TS. Moreover, having similar q_{calc} and q_{exp} values further confirms that the adsorption mechanism follows the pseudo–second-order kinetics. In order to examine the diffusion mechanism, the kinetic data were applied with the intra-particle diffusion model. Adsorption mechanism can be described in several steps such as film or bulk diffusion, particle or surface diffusion, intra-particle or pore diffusion, and adsorption on the active centers in the interior side of the adsorbent [35]. If the rate-controlling step in adsorption is the intra-particle diffusion, then the plot of q_t vs. $t^{1/2}$ should be a straight line and pass through the origin. In this study, intra-particle diffusion could not be the only rate-determining step as indicated by the y-intercept (C) value. Therefore, it could be said that the adsorption process may

Table 6
Thermodynamics parameters

T (K)	ln K_c	ΔG° (kJ mol^{-1})	ΔS° (J mol^{-1} K^{-1})	ΔH (kJ mol^{-1})
TS				
298	1.05	−2.6	109.4	29.7
314	1.76	−4.6		
324	2.32	−6.2		
334	2.33	−6.4		
344	2.64	−7.5		
NaOH-TS				
298	4.68	−11.96	97.2	17.5
314	4.83	−12.56		
324	5.10	−13.69		
334	5.50	−15.23		
344	5.50	−15.69		

involve more than one step. The value of C is directly proportional to the boundary layer thickness; higher the value of C, more will be the thickness and film resistance. Comparing parameters observed for TS and NaOH-TS, it was found that NaOH-TS had higher rate of diffusion (k_{id}) than TS. It could be due to less film resistance for adsorption of CV onto NaOH-TS as indicated by lower boundary layer thickness (C) value. The Elovich plot of $ln\ t$ vs q_t gives a linear relationship. With correlation coefficient (R^2) value > 0.96, the Elovich model is successfully applied for CV adsorption onto TS and NaOH-TS. The Elovich model supports the heterogeneous sorption mechanism for the dye uptake involving a variation of the energetic of chemisorption with the active sites in adsorbents [36].

3.7. Adsorption thermodynamics

The extent of equilibrium at different solution temperatures would be of importance if real treatment procedures are employed at warmer temperatures. In this respect, thermodynamic parameters would provide necessary importance in designing effluent treatment plants. The standard Gibbs free energy change (ΔG°), standard enthalpy change (ΔH°), and standard entropy change (ΔS°) can be given by the following standard equations:

$$\Delta G^\circ = RT \ln K_c \quad \text{and } K_c = C_a/C_e \tag{17}$$

$$\text{Van't Hoff equation: } \ln K_c = \frac{\Delta H^\circ}{RT} = \frac{\Delta S^\circ}{R} \tag{18}$$

where K_c is the distribution coefficient, C_a is the dye concentration (mg L^{-1}) on the adsorbent at equilibrium, and C_e is the equilibrium dye concentration in solution (mg L^{-1}).

The Gibbs free energy values calculated at different temperatures for adsorption of CV on both types of TS samples are listed in Table 6. Positive values of ΔH° from ln K_c vs. $1/T$ plot (Fig. 13) indicate that adsorption of CV on TS and NaOH-TS is endothermic in nature. The positive entropy changes (ΔS°) reflect good affinity of dye molecules toward adsorbents. Negative ΔG° values provide the most important condition that the system under investigation is spontaneous. The spontaneity improves at warmer temperature which is supported form the endothermic nature of adsorption indicated by enthalpy changes. This factor should be considered in expanding the use of such natural adsorbents for treatment of real effluents.

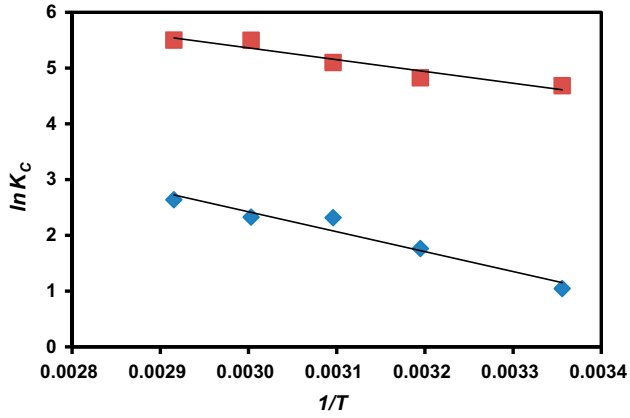

Fig. 13. ln K_c vs. $1/T$ plot for evaluation of ΔH° and ΔS°: TS (♦) and NaOH-TS (■).

4. Conclusion

A. odoratissimus peel (TS) is an efficient adsorbent for CV having a capacity of 118 mg g^{-1} under optimized experimental conditions of 2.5 h shaking time and 30 min settling time at ambient pH according to the Langmuir adsorption isotherm. Treatment of TS with 1.0 M NaOH enhances the extent of adsorption by about 65%, which is a great achievement. This is probably due to the deprotonation of carboxylic and phenolic groups present in the adsorbent promoting attraction with positively charged dye molecules. Having R^2, value close to unity, it is proposed that kinetics of adsorption of CV on TS and NaOH-TS fulfil pseudo-second-order and Weber–Morris intra-particle model for diffusion of CV species toward the adsorbent matrix. The process is thermodynamically favorable, spontaneous, and accompanied by an increase in randomness. The results of this research can be of importance in designing large-scale treatment facilities for wastewater containing dyes.

Acknowledgment

The authors would like to thank the Government of Brunei Darussalam and the Universiti Brunei Darussalam (UBD) for their financial support. The authors are also grateful to the Centre for Advanced Material and Energy Sciences (CAMES) and the Department of Biology at UBD for the use of XRF and SEM, respectively.

References

[1] P.V. Nidheesh, R. Gandhimathi, S.T. Ramesh, Degradation of dyes from aqueous solution by Fenton processes: A review, Environ. Sci. Pollut. Res. 20 (2013) 2099–2132.

[2] O. Ganzenko, D. Huguenot, E.D. van Hullebusch, G. Esposito, M.A. Oturan, Electrochemical advanced oxidation and biological processes for wastewater treatment: A review of the combined approaches, Environ. Sci. Pollut. Res. 21 (2014) 8493–8524.
[3] N. Priyantha, L.B.L. Lim, M.K. Dahri, D.T.B. Tennakoon, Dragon fruit skin as a potential low-cost biosorbent for the removal of Manganese(II) ions, J. Appl. Sci. Environ. Sani. 8 (2013) 179–188.
[4] H.I. Chieng, L.B.L. Lim, N. Priyantha, Enhancing adsorption capacity of toxic malachite green dye through chemically modified breadnut peel: Equilibrium, thermodynamics, kinetics and regeneration studies, Environ. Technol. 36 (2015) 86–97.
[5] T. Zehra, N. Priyantha, L.B.L. Lim, E. Iqbal, Sorption characteristics of peat of Brunei Darussalam V: Removal of Congo red dye from aqueous solution by peat, Desalin. Water Treat. (2014), doi: 10.1080/19443994.2014.899929.
[6] M.K. Dahri, M.R.R. Kooh, L.B.L. Lim, Removal of methyl violet 2B from aqueous solution using *Casuarina equisetifolia* needle, ISRN Environ. Chem. Available from: <http://dx.doi.org/10.1155/2013/619819>.
[7] P. Pandey, R.P. Singh, K.N. Singh, P. Manisankar, Evaluation of the individuality of white rot macro fungus for the decolorization of synthetic dye, Environ. Sci. Pollut. Res. 20 (2013) 238–249.
[8] G. Boduroğlu, N.K. Kılıç, G. Dönmez, Bioremoval of Reactive Blue 220 by Gonium sp. biomass, Environ. Technol. 35 (2014) 2410–2415.
[9] A. Azhdarpoor, R. Nikmanesh, F. Khademi, A study of Reactive Red 198 adsorption on iron filings from aqueous solutions, Environ. Technol. 35 (2014) 2956–2960.
[10] Y.P. Tang, L.B.L. Lim, L.W. Franz, Proximate analysis of *Artocarpus odoratissimus* (Tarap) in Brunei Darussalam, Int. Food Res. J. 20 (2013) 409–415.
[11] L.B.L. Lim, N. Priyantha, D.T.B. Tennakoon, M.K. Dahri, Biosorption of cadmium(II) and copper(II) ions from aqueous solution by core of *Artocarpus odoratissimus*, Environ. Sci. Pollut. Res. 19 (2012) 3250–3256.
[12] L.B.L. Lim, N. Priyantha, H.I. Chieng, M.K. Dahri, D.T.B. Tennakoon, T. Zehra, M. Suklueng, Artocarpus odoratissimus skin as a potential low-cost biosorbent for the removal of methylene blue and methyl violet 2B, Desalin. Water Treat. 53 (2015) 964–975.
[13] L.B.L. Lim, N. Priyantha, N.H.M. Mansor, Artocarpus altilis (breadfruit) skin as a potential low-cost biosorbent for the removal of crystal violet dye: Equilibrium, thermodynamics and kinetics studies, Environ. Earth Sci. 73 (2015) 3239–3247.
[14] M. Alshabana, G. Alsenani, R. Almufarij, Removal of crystal violet dye from aqueous solutions onto date palm fiber by adsorption technique, J. Chem. (2013), doi: 10.1155/2013/210239.
[15] T. Chinniagounder, M. Shanker, S. Nageswaran, Adsorptive removal of crystal violet dye using agricultural waste Cocoa (*Theobroma cacao*) shell, Res. J. Chem. Sci. 1 (2011) 38–45.
[16] P.D. Saha, S. Chakraborty, S. Chowdhury, Batch and continuous (fixed-bed column) biosorption of crystal violet by *Artocarpus heterophyllus* (jackfruit) leaf powder, Colloids Surf., B 92 (2012) 262–270.
[17] S. Chakraborty, S. Chowdhury, P. Das Saha, Biosorption of hazardous textile dyes from aqueous solutions by hen feathers: Batch and column studies, Korean J. Chem. Eng. 29 (2012) 1567–1576.
[18] S. Chowdhury, S. Chakraborty, P.D. Saha, Removal of crystal violet from aqueous solution by adsorption onto eggshells: Equilibrium, kinetics, thermodynamics and artificial neural network modeling, Waste Biomass Valor. 4 (2013) 655–664.
[19] J. Široký, R.S. Blackburn, T. Bechtold, J. Taylor, P. White, Alkali treatment of cellulose II fibres and effect on dye sorption, Carbohydr. Polym. 84 (2011) 299–307.
[20] A. Ebrahimian Pirbazari, E. Saberikhah, M. Badrouh, M.S. Emami, Alkali treated Foumanat tea waste as an efficient adsorbent for methylene blue adsorption from aqueous solution, Water Res. Industry 6 (2014) 64–80.
[21] S. Chowdhury, S. Chakraborty, P.D. Saha, Adsorption of crystal violet from aqueous solultion by citric acid modified rice straw: Equilibrium, kinetics, and thermodynamics, Sep. Sci. Technol. 48 (2013) 1339–1348.
[22] S. Chakraborty, S. Chowdhury, P.D. Saha, Batch removal of crystal violet from aqueous solution by H_2SO_4 modified sugarcane bagasse: Equilibrium, kinetic, and thermodynamic profile, Sep. Sci. Technol. 47 (2012) 1898–1905.
[23] H.Y. Huo, H.J. Su, W. Jiang, T.W. Tan, Effect of Ag^+ adsorption on degradation of organic dye waste, Biochem. Eng. J. 43 (2009) 2–7.
[24] M. Dogan, Y. Ozdemir, M. Alkan, Adsorption kinetics and mechanism of cationic methyl violet and methylene blue dyes onto sepiolite, Dyes Pigments 75 (2009) 701–713.
[25] N. Tekin, Ö. Demirbaş, M. Alkan, Adsorption of cationic polyacrylamide onto kaolinite, Microporous Mesoporous Mater. 85 (2005) 340–350.
[26] H.I. Chieng, L.B.L. Lim, N. Priyantha, D.T.B. Tennakoon, Sorption characteristics of peat of Brunei Darussalam III: Equilibrium and kinetics studies on adsorption of crystal violet (CV), Int. J. Earth Sci. Eng. 6 (2013) 791–801.
[27] S. Chakraborty, S. Chowdhury, P. Das Saha, Adsorption of crystal violet from aqueous solution onto NaOH-modified rice husk, Carbohydr. Polym. 86 (2011) 1533–1541.
[28] L. Zhang, H. Zhang, W. Guo, Y. Tian, Removal of malachite green and crystal violet cationic dyes from aqueous solution using activated sintering process red mud, Appl. Clay Sci. 93–94 (2014) 85–93.
[29] S. Senthilkumaar, P. Kalaamani, C.V. Subburaam, Liquid phase adsorption of crystal violet onto activated carbons derived from male flowers of coconut tree, J. Hazard. Mater. 136 (2006) 800–808.
[30] G.O. El-Sayed, Removal of methylene blue and crystal violet from aqueous solutions by palm kernel fiber, Desalination 272 (2011) 225–232.
[31] R. Kumar, R. Ahmad, Biosorption of hazardous crystal violet dye from aqueous solution onto treated ginger waste (TGW). Desalination 265 (2011) 112–118.
[32] F.A. Pavan, E.S. Camacho, E.C. Lima, G.L. Dotto, V.T.A. Branco, S.L.P. Dias, Formosa papaya seed powder (FPSP): Preparation, characterization and application as an alternative adsorbent for the removal

of crystal violet from aqueous phase, J. Environ. Chem. Eng. 2 (2014) 230–238.
[33] K.P. Singh, S. Gupta, A.K. Singh, S. Sinha, Optimizing adsorption of crystal violet dye from water by magnetic nanocomposite using response surface modeling approach, J. Hazard. Mater. 186 (2011) 1462–1473.
[34] G.R. Mahdavinia, A. Massoudi, A. Baghban, E. Shokri, Study of adsorption of cationic dye on magnetic kappa-carrageenan/PVA nanocomposite hydrogels, J. Environ. Chem. Eng. 2 (2014) 1578–1587.
[35] O.M. Paşka, C. Păcurariu, S.G. Muntean, Kinetic and thermodynamic studies on methylene blue biosorption using corn-husk, RSC Adv. 4 (2014) 62621–62630.
[36] N. Renugadevi, R. Sangeetha, P. Lalitha, Kinetics of the adsorption of methylene blue form an industrial dyeing effluent onto activated carbon, prepared from the fruits of *Mimuops elengi*, Appl. Sci. Res. 3 (2011) 492–498.